


RESEARCH ARTICLE

Folate receptor α increases chemotherapy resistance through stabilizing MDM2 in cooperation with PHB2 that is overcome by MORAb-202 in gastric cancer

Hitomi Sakai¹ | Hisato Kawakami¹  | Takeshi Teramura² | Yuta Onodera²  | Elizabeth Somers³ | Keiji Furuuchi⁴ | Toshimitsu Uenaka⁴ | Ryoji Kato¹ | Kazuhiko Nakagawa¹

¹ Department of Medical Oncology, Kindai University Faculty of Medicine, Osaka-Sayama, Osaka, Japan

² Division of Cell Biology for Regenerative Medicine, Institute of Advanced Clinical Medicine, Kindai University Faculty of Medicine, Osaka-Sayama, Osaka, Japan

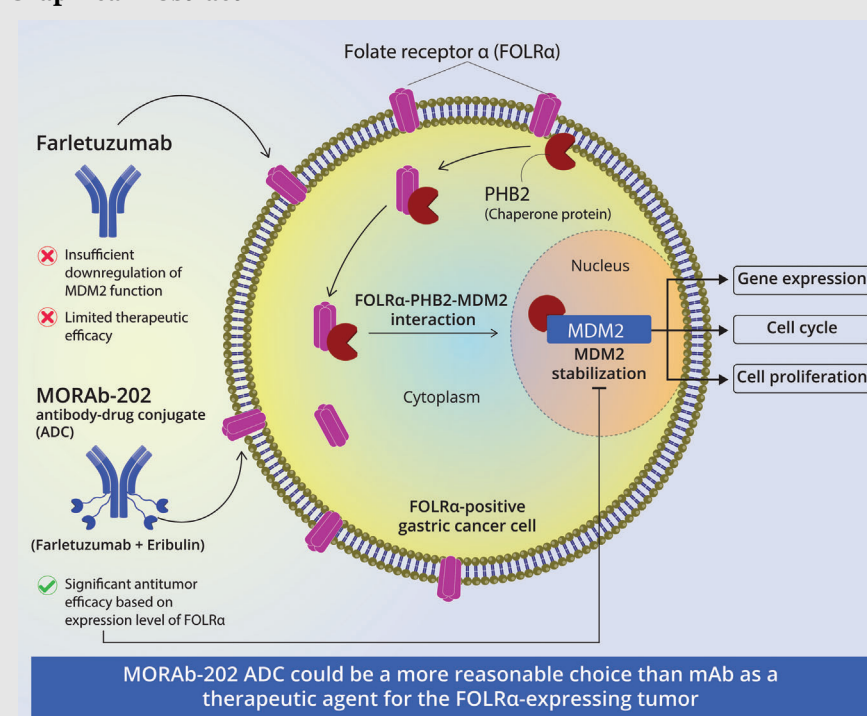
³ AD Franchise Special Mission, Eisai Inc., Woodcliff Lake, New Jersey, USA

⁴ Epochal Precision Anti-Cancer Therapeutics (EPAT), Eisai Inc., Exton, Pennsylvania, USA

Correspondence

*Hisato Kawakami, Department of Medical Oncology, Kindai University Faculty of Medicine, 377-2 Ohno-higashi, Osaka-Sayama, Osaka 589-8511, Japan.
Email: kawakami_h@med.kindai.ac.jp

Graphical Abstract



1. MDM2 may determine the malignant phenotype of FOLR α -expressing cancers as a result of the FOLR α -PHB2-MDM2 axis.
2. The anti-FOLR α monoclonal antibody farletuzumab did not suppress the MDM2-mediated chemotherapy resistance and cell proliferation in gastric cancer cells.
3. The antitumor efficacy of MORAb-202, a farletuzumab-eribulin antibody-drug conjugate, for gastric cancer cell lines depended on the level of FOLR α expression.

RESEARCH ARTICLE

Folate receptor α increases chemotherapy resistance through stabilizing MDM2 in cooperation with PHB2 that is overcome by MORAb-202 in gastric cancer

Hitomi Sakai¹ | Hisato Kawakami¹  | Takeshi Teramura² | Yuta Onodera²  | Elizabeth Somers³ | Keiji Furuuchi⁴ | Toshimitsu Uenaka⁴ | Ryoji Kato¹ | Kazuhiko Nakagawa¹

¹ Department of Medical Oncology, Kindai University Faculty of Medicine, Osaka-Sayama, Osaka, Japan

² Division of Cell Biology for Regenerative Medicine, Institute of Advanced Clinical Medicine, Kindai University Faculty of Medicine, Osaka-Sayama, Osaka, Japan

³ AD Franchise Special Mission, Eisai Inc., Woodcliff Lake, New Jersey, USA

⁴ Epochal Precision Anti-Cancer Therapeutics (EPAT), Eisai Inc., Exton, Pennsylvania, USA

Correspondence

*Hisato Kawakami, Department of Medical Oncology, Kindai University Faculty of Medicine, 377-2 Ohno-higashi, Osaka-Sayama, Osaka 589-8511, Japan.

Email: kawakami_h@med.kindai.ac.jp

Funding information

Eisai Incorporated.

Abstract

Background: The main function of folate receptor α (FOLR α) has been considered to mediate intracellular folate uptake and induce tumor cell proliferation. Given the broad spectrum of expression among malignant tumors, including gastric cancer (GC) but not in normal tissue, FOLR α represents an attractive target for tumor-selective drug delivery. However, the efficacy of anti-FOLR α monoclonal antibodies (mAbs) has not been proved so far, with the reason for this failure remaining unclear, raising the need for a better understanding of FOLR α function.

Methods: The distribution of FOLR α in GC cells was evaluated by immunohistochemistry. The impacts of FOLR α expression on the survival of GC patients and GC cell lines were examined with the Gene Expression Omnibus database and by siRNA of FOLR α . RNA-sequencing and Microarray analysis was conducted to identify the function of FOLR α . Proteins that interact with FOLR α were identified with shotgun LC-MS/MS. The antitumor efficacy of the anti-FOLR α mAb farletuzumab as well as the antibody-drug conjugate (ADC) consists of the farletuzumab and the tubulin-depolymerizing agent eribulin (MORAb-202) was evaluated both *in vitro* and *in vivo*.

Results: FOLR α was detected both at the cell membrane and in the cytoplasm. Shorter overall survival was associated with FOLR α expression in GC patients, whereas reduction of FOLR α attenuated cell proliferation without inducing cell

Abbreviations: ADC, antibody-drug conjugate; EMT, epithelial mesenchymal transition; ERK, extracellular signal-regulated Kinase; FACS, fluorescence-activated cell sorting; FBS, fetal bovine serum; FCS, Fetal Calf Serum; FITC, fluorescein isothiocyanate; FOLR α , folate receptor α ; GC, gastric cancer; GEO, gene expression omnibus; GO, gene ontology; GPI, glycosylphosphatidylinositol; HRP, horseradish peroxidase; LC-MS/MS, liquid chromatography tandem mass spectrometry; mAb, monoclonal antibody; MAPK, mitogen-activated protein kinase; PHB1, prohibitin1; PHB2, prohibitin2; RT-qPCR, reverse transcription-quantitative polymerase chain reaction

This is an open access article under the terms of the [Creative Commons Attribution](https://creativecommons.org/licenses/by/4.0/) License, which permits use, distribution and reproduction in any medium, provided the original work is properly cited.

© 2021 The Authors. *Clinical and Translational Medicine* published by John Wiley & Sons Australia, Ltd on behalf of Shanghai Institute of Clinical Bioinformatics

death in GC cell lines. Transcriptomic and proteomic examinations revealed that the FOLR α -expressing cancer cells possess a mechanism of chemotherapy resistance supported by MDM2, and FOLR α indirectly regulates it through a chaperone protein prohibitin2 (PHB2). Although reduction of FOLR α brought about vulnerability for oxaliplatin by diminishing MDM2 expression, farletuzumab did not suppress the MDM2-mediated chemoresistance and cell proliferation in GC cells. On the other hand, MORAb-202 showed significant antitumor efficacy.

Conclusions: The ADC could be a more reasonable choice than mAb as a targeting agent for the FOLR α -expressing tumor.

KEYWORDS

antibody-drug conjugate, folate receptor α (FOLR α), gastric cancer, MDM2

1 | INTRODUCTION

Gastric cancer is the fifth most common cancer type and the third leading cause of cancer deaths worldwide.¹ Given the limited number of selective and effective molecularly targeted agents available for gastric cancer, the identification of new target molecules is urgently needed.

Folate receptor α (FOLR α) is a 38-kDa glycosylphosphatidylinositol (GPI)-linked cell-surface glycoprotein encoded by the gene *FOLR1*. FOLR α binds folate with high affinity and mediates its cellular uptake.² FOLR α is expressed in various tumor types, including ovarian, endometrial, non-small cell lung, and triple-negative breast cancers, whereas its expression at a substantial level in normal tissues is essentially limited to the kidney, choroid plexus, placenta, and lung.³ This expression pattern—high expression in a broad spectrum of solid tumors and low expression in normal tissue—has led to an interest in FOLR α as a potential therapeutic target. Indeed, FOLR α -targeting agents have been preceded by treatment of patients with the four malignancies with the highest rates of FOLR α overexpression: ovarian, endometrial, triple-negative breast, and non-small cell lung cancer.⁴ Gastric cancer can be another candidate of anti-FOLR α therapy given a substantial rate of FOLR α expression.⁵

Among FOLR α -targeting agents, farletuzumab, a humanized monoclonal antibody (mAb), is the most advanced in clinical development. In a phase III study of platinum-sensitive ovarian cancer, however, the addition of farletuzumab to carboplatin plus either paclitaxel or docetaxel failed to improve treatment outcome, with the reason for this failure remaining unclear.⁴ Nonetheless, the concept of FOLR α -targeted therapy continues to be explored with multiple anti-FOLR α agents—including MORAb-202, an antibody-drug conjugate (ADC) consisting of farletuzumab and the tubulin inhibitor eribulin

mesylate—with some of these agents have entered clinical trials.⁴ A better understanding of FOLR α function would facilitate the development of such therapy.

We have now studied the role of FOLR α in gastric cancer and found that a signaling axis comprising FOLR α , prohibitin 2 (PHB2), and murine double minute 2 (MDM2) contributes to chemotherapy resistance. We further found that this resistance mechanism could be overcome by MORAb-202, although not by farletuzumab plus chemotherapy. Together with the substantial frequency of FOLR α expression in gastric cancer, our results suggest that FOLR α is indeed a feasible therapeutic target for gastric tumors.

2 | METHODS

2.1 | Cells and reagents

The human gastric cancer cell lines MKN1 (RRID, CVCL_1415), MKN74 (CVCL_2791), MKN45 (CVCL_0434), and NUGC3 (CVCL_1612), as well as HeLa cervical carcinoma cells (CVCL_0030), were obtained from the JCRB cell bank. The human gastric cancer cell lines SNU1 (CVCL_0099), Hs746T (CVCL_0333), and NCI-N87 (CVCL_1603) were from American Type Culture Collection and SNU216 (CVCL_3946) was from the Korean Cell Line Bank. The cells were maintained under a humidified atmosphere of 5% CO₂ at 37°C in RPMI 1640 medium (Sigma-Aldrich) supplemented with 10% heat-inactivated fetal bovine serum (FBS) (Biowest) and 1% penicillin-streptomycin-amphotericin B (Wako). Cells were tested for mycoplasma contamination using MycoAlert (LT07, Lonza) and were confirmed negative. Eribulin was obtained from Eisai Co. Ltd and Oxaliplatin from Yakult. MORAb-202 and farletuzumab were provided by Eisai Co. Ltd. MG132 was obtained from Funakoshi.

TABLE 1 Sequences of PCR primers, guide RNAs, and siRNAs used in this study

RT-qPCR primers	Forward (5'-3')	Reverse (5'-3')
<i>FOLR1</i>	TTCATCCAGGACACCTGCCTC	ATTGCTCACAGTCCTCTTTGC
<i>MDM2</i>	AACAGGTGTCACCTTGAAGGTG	TGAGGTAGATGGTCTAGAAACC
<i>GAPDH</i>	TGGTAAAGTGGATATTGTTGC	TTCTCAGCCTTGACGGTGC
Genotyping PCR primers		
<i>FOLR1</i>	TCAGGTGATCCACCCACCTC	AGATCTTTGGAGGAGTCATTC
Guide RNAs		
	Sense (5'-3')	Antisense (5'-3')
FOLR1-1	ACACC ACCTGAACCTCGTGACCACC G	AAAAC GTGGTCACGAGGTTTCAGGTC G
FOLR1-2	ACACC GTTGGCATTGTACCGACATT G	AAAAC AATGTCCGGTACAATGCCAAC G
siRNAs		
<i>FOLR1</i>	GGA UGU UUC CUA CCU AUA UdTdT	AUA UAG GUA GGA AAC AUC CdTdT
<i>MDM2</i>	GAA AAU UCA GAU GAA UUA UdTdT	AUA AUU CAU CUG AAU UUU CdTdT
<i>PHB1</i>	GCA AAG AUU UAC AGA AUG UdTdT	ACA UUC UGU AAA UCU UUG CdTdA
<i>PHB2</i>	CAG AAU CGU AUC UAU CUC AdTdT	UGA GAU AGA UAC GAU UCU GdTdT
Scrambled	GUA CUC AUG CUA UAU UGC UdTdT	AGC AAU AUA GCA UGA GUA CdTdT

2.2 | Antibodies and primers

Sequences of PCR primers, guide RNAs, and siRNAs used in this study are shown in Table 1. Antibodies and dilution conditions are shown in Table 2.

2.3 | Animal use and care

All animal experiments were performed following the Recommendations for Handling of Laboratory Animals for Biomedical Research compiled by the Committee on Safety and Ethical Handling Regulations for Laboratory Animal Experiments, Kindai University. The study was also approved by the Animal Ethics Committee of Kindai University. Female BALB/CAJcl-nu/nu mice (CLEA Japan) were housed in groups of four or five with food and water available *ad libitum*, and they were exposed to an artificial light-dark regimen with 14 h of light and 10 h of darkness and to a temperature maintained between 20°C and 25°C in a ventilated room.

2.4 | Immunohistochemistry method for staining and interpretation of results in the formalin-fixed, paraffin-embedded whole tissue sections to evaluate the frequency of expression in the Tumor Scan Study

FOLR α expression levels were determined using the FRA-26B3 IHC assay kit manufactured by Biocare Medical, Inc. and stained using the Biocare IntelliPath Automated

Slide Stainer. The following assay procedure was utilized for staining endometrial, gastric, triple-negative breast cancer, non-small cell lung adenocarcinoma, and ovarian carcinoma formalin-fixed, paraffin-embedded tissue sections. Following incubation with the primary monoclonal antibody to human FOLR α protein or the negative control reagent, a rabbit anti-mouse secondary polyclonal antibody was used to detect the primary antibody, and horseradish peroxidase (HRP)-labeled goat polyclonal anti-rabbit micro-polymer was used to recognize the rabbit immunoglobulin present in the secondary antibody. The subsequently added 3,3'-diaminobenzidine chromogen is converted by the HRP enzyme of the micro-polymer into a visible reaction product (brown precipitate) at the antigen site. The specimens were counterstained, dehydrated, cleared, and cover-slipped for scoring and interpretation by a board-certified anatomic pathologist using a light microscope.

Interpretation of FOLR α expression levels was accomplished using specific criteria for evaluation. Each slide was evaluated for both the percentage of membrane and cytoplasm stained and the intensity of staining. Results of cytoplasmic and membranous expression levels were both recorded. Negative expression levels were scored as 0, for no staining present; 1+, for weak staining; 2+, for moderate and 3+, for strong staining. Only tumor cells were scored. FOLR α positivity was defined as membrane staining greater than or equal to 5% of neoplastic cells at any intensity level. Cytoplasmic staining levels were evaluated and recorded for use in the evaluation and characterization of staining; however, they were not utilized in the determination of percent positive results included in the tumor expression figure.

TABLE 2 Antibodies and dilution conditions

Antibodies	Company	Application	Dilution
PHB1 (#2426)	Cell Signaling Technology	IB	1/1000 in Immunoenhancer
PHB2 (E1Z5A, #14085)	Cell Signaling Technology	IB	1/1000 in Immunoenhancer
p53 (#9282)	Cell Signaling Technology	IB	1/5000 in TBS containing 0.2% Tween-20 and 10% Block Ace
MDM2 (D1V2Z, #86934)	Cell Signaling Technology	IB	1/1000 in Immunoenhancer
Rb (D20, 9313)	Cell Signaling Technology	IB	1/1000 in Immunoenhancer
Phospho-histone H3 (Ser ¹⁰) (#3377, D2C8)	Cell Signaling Technology	IB	1/1000 in Immunoenhancer
Phospho-Wee1 (Ser ⁶⁴²) (#4910, D47G5)	Cell Signaling Technology	IB	1/1000 in Immunoenhancer
CDK2 (#2546, 78B2)	Cell Signaling Technology	IB	1/1000 in Immunoenhancer
CDK4 (#12790, D9G3E)	Cell Signaling Technology	IB	1/1000 in Immunoenhancer
CDK6 (#3136, DCS83)	Cell Signaling Technology	IB	1/1000 in Immunoenhancer
Myt1 (#4282)	Cell Signaling Technology	IB	1/1000 in Immunoenhancer
p27(Kip1) (#3686, D69C12)	Cell Signaling Technology	IB	1/1000 in Immunoenhancer
Cyclin D3 (#2936, DCS22)	Cell Signaling Technology	IB	1/1000 in Immunoenhancer
p21(Waf1/Cip1) (#2947, 12D1)	Cell Signaling Technology	IB	1/1000 in Immunoenhancer
Cyclin A2 (#4656, BF683)	Cell Signaling Technology	IB	1/1000 in Immunoenhancer
Cyclin B1 (#12231, D5C10)	Cell Signaling Technology	IB	1/1000 in Immunoenhancer
Phospho-CDC2 (Tyr ¹⁵) (#4539, 10A11)	Cell Signaling Technology	IB	1/1000 in Immunoenhancer
Cyclin E2 (#4132)	Cell Signaling Technology	IB	1/1000 in Immunoenhancer
p18(Ink4c) (#2896, DCS118)	Cell Signaling Technology	IB	1/1000 in Immunoenhancer
Cyclin D1(#2978, 92G2)	Cell Signaling Technology	IB	1/1000 in Immunoenhancer
Phospho-GSK3 β (Ser ⁹) (#9323, 5B3)	Cell Signaling Technology	IB	1/1000 in Immunoenhancer
EP300 (#86377, D8Z4E)	Cell Signaling Technology	IB	1/1000 in Immunoenhancer
FOLR α (NCL-L-FR α)	Leica	IB	1/1000 in Immunoenhancer
Phospho-ATM (Ser ¹⁹⁸¹) (2152-1)	Epitomics	IB	1/1000 in Immunoenhancer
GAPDH (016-25523, 5A12)	FujiIFilm Wako	IB	1/1000 in Immunoenhancer
HRP-conjugated goat anti-mouse IgG (G0407)	Tokyo Chemical Industry	IB	1/1000 in Immunoenhancer
HRP-conjugated goat anti-rabbit IgG (G0418)	Tokyo Chemical Industry	IB	1/1000 in Immunoenhancer
Phospho p38 (Thr180/Tyr182, #4511)	Cell Signaling Technology	IB	1/3000 in Immuno-enhancer
p38 (#9212)	Cell Signaling Technology	IB	1/5000 in Immuno-enhancer
Phospho Erk1/2	Cell Signaling Technology	IB	1/3000 in Immuno-enhancer
Erk1/2 (#4695)	Cell Signaling Technology	IB	1/5000 in Immuno-enhancer
Phospho Akt (Ser473, #4060)	Cell Signaling Technology	IB	1/3000 in Immuno-enhancer
Akt (#9272)	Cell Signaling Technology	IB	1/5000 in Immuno-enhancer
Caspase-3 (#9662)	Cell Signaling Technology	IB	1/3000 in Immuno-enhancer
FOLR α (NCL-L-FR α)	Leica	IP for IB	3 μ g
MDM2 (sc-813, N-20)	Santa Cruz Biotechnology	IP for IB	3 μ g
Normal human IgG (143-09501)	FujiFilm Wako	IP for IB	3 μ g
Normal rabbit IgG (PM035)	MBL	IP for IB	3 μ g
FOLR α (NCL-L-FR α)	Leica	IP for MS	1 μ g
Normal human IgG (143-09501)	FujiFilm Wako	IP for MS	1 μ g
FOLR α (NCL-L-FR α)	Leica	Flow cytometry /FACS	10 μ g/mL

Abbreviations. IB, immunoblot analysis; IP, immunoprecipitation; MS, mass spectrometry; FACS, fluorescence-activated cell sorting.

2.5 | Propidium iodide staining

Cells were transfected with *siFOLR α* or treated with oxaliplatin (L-OHP) for 48 h. Cells were incubated with propidium iodide (PI) at a concentration of 0.1 mg/ml in 0.01 M phosphate-buffered saline (PBS), pH 7.2, for 30 min at room temperature in the dark. Cells were thoroughly washed in PBS, mounted in glycerol, and observed under a fluorescence microscope.

2.6 | Immunofluorescence analysis

Cells were fixed for 30 min at room temperature with 10 N Mildform (Wako), washed three times with TBS containing 0.1% Tween-20, incubated for 30 min in Block Ace, and washed again twice before exposure overnight at 4°C to antibodies to FOLR α . The cells were washed another three times, incubated for 60 min at room temperature with fluorescein isothiocyanate (FITC)-conjugated secondary antibodies, and then stained with DAPI before observation with a BZX-710 microscope (Keyence).

2.7 | Cell counts

Cells were plated at a density of 5×10^4 per well of a 24-well plate and incubated for the indicated times with the indicated agents, that is, oxaliplatin or eribulin for 24 h. The cells were then isolated as single-cell suspensions by exposure to trypsin, and they were counted with a hemocytometer after staining with trypan blue (Thermo Fisher Scientific).

2.8 | In vitro cell viability assay

Cells were plated in 96-well flat-bottomed plates at a density of 1200 to 6000 per well depending on the cell line in RPMI 1640 medium supplemented with 10% FBS. After culturing for 24 h, the cells were exposed to various concentrations of MORAb-202 for 120 h, and cell viability was then assessed with the use of a Cell Counting Kit-8 (Promega).

2.9 | Reverse transcription-quantitative polymerase chain reaction analysis

Total RNA was extracted from cells using the TRIzol reagent (Molecular Research Center) and was subjected to RT with a PrimeScript RT Master Mix Kit (Takara Bio). The resulting cDNA was subjected to real-time PCR

analysis with the use of a Thermal Cycler Dice Real Time System Single, with incubation at 95°C for 20 s followed by 40 cycles of 95°C for 5 s and 60°C for 30 s. For quantitation of relative gene expression, the threshold cycle (Ct) values were normalized by that for the housekeeping gene GAPDH and were then calibrated with the $\Delta\Delta C_t$ method. Amplification of contaminating genomic DNA was limited with the use of primers designed to span at least one intron. Primer sequences are listed in Table 1.

2.10 | Immunoblot analysis

Cells were homogenized in SDS sample buffer [4% SDS, 125 mM Tris-glycine, 10% β -mercaptoethanol, and 2% bromophenol blue in 30% glycerol], the homogenate was centrifuged at 15,000 rpm at 4°C for 10 min to remove debris, and portions of the resulting supernatant were subjected to SDS-PAGE. The separated proteins were transferred to a polyvinylidene difluoride membrane (GE Healthcare), which was then exposed overnight at room temperature to Block Ace (Dainippon Sumitomo Pharma) before incubation overnight at 4°C with primary antibodies. Immune complexes were detected with horseradish peroxidase-conjugated secondary antibodies and Immunostar LD (Wako) reagents. All antibodies used are listed in Table 2.

2.11 | Co-immunoprecipitation analysis

Cells were lysed in IP extraction buffer [25 mM Tris-HCl (pH 7.5), 100 mM NaCl, 0.5% Triton X-100] for 30 min on ice, the lysate was centrifuged to remove debris, and the resulting supernatant was incubated overnight at 4°C with primary antibodies conjugated to Dynabeads Protein G (Veritas) in Tris-buffered saline (TBS) containing 0.02% Tween-20. The precipitated proteins were eluted in an SDS sample buffer for immunoblot analysis. All antibodies used are listed in Supplementary Table 2.

2.12 | Liquid chromatography-tandem mass spectrometry analysis

HeLa cells were fixed for 10 min at room temperature with 0.1% formaldehyde (Wako) and then lysed with a modified RIPA buffer consisting of 20 mM HEPES-NaOH (pH 7.5), 1 mM EGTA, 1 mM MgCl₂, 150 mM NaCl, 0.25% sodium deoxycholate, 0.05% SDS, 1% Nonidet P-40, PhosSTOP (Merck, #4906845001), and Benzodase (1/500; Merck, #E1014). The lysate was subjected to immunoprecipitation as described above. The immunoprecipitate

was collected in the modified RIPA buffer and was subjected to alkylation followed by digestion overnight at 37°C with Lys-C (4 µg/ml) and Mass Spec Grade Trypsin (Promega). After desalting with GL-Tip SDB (GL Sciences, #7820-11200), the sample was concentrated with the use of a SpeedVac (Thermo Fisher Scientific), and its peptide concentration was determined with a Pierce Quantitative Colorimetric Peptide Assay Kit (Thermo Fisher Scientific, #23275). Peptides were fractionated with the use of a HyperSep Retain CX column and ammonium acetate. The fractions were then desalted with a C18 before analysis with Orbitrap Fusion Lumos and Q Exactive HF mass spectrometers. Spectral data files were analyzed with XlinkX 2.0 and Proteome Discover 2.2 software with the use of XlinkX node and SEQUEST HT. Binding proteins with a high confidence level (206 proteins) were selected from the raw data on the basis of the false discovery rate. Ribosomal proteins were then excluded, and the function of the remaining proteins (188 molecules) was examined by WikiPathway analysis. Sequential selection of proteins whose function is related to cell proliferation or cell survival and of proteins that are localized to the cell membrane or cytoplasm yielded 53 and 20 proteins.

2.13 | RNA interference

Transfection of cells with siRNAs was performed with the use of the Lipofectamine RNAiMAX reagent (Thermo Fisher Scientific). The sequences of the siRNAs are provided in Table 1. Knockdown efficiency was confirmed by reverse transcription-quantitative polymerase chain reaction (RT-qPCR) or immunoblot analysis.

2.14 | CRISPR/CAS9

For the CRISPR-Cas9 treatment, MKN1 was dissociated with TrypLE Express, washed twice with Opti-MEM, and resuspended in 100 µL of Opti-MEM containing 7.5 µg of MLM3636 guide RNA expression plasmids and 5 µg Cas9 expression plasmid. MLM3636 plasmid was a gift from Dr. Keith Joung (Addgene plasmid # 43860) and pSpCas9(BB)-2A-Puro (PX459) V2.0 was a gift from Dr. Feng Zhang (Addgene plasmid # 62988). After 1 µg/µL puromycin selection for 10 days, the resulting colonies were cloned into the 96 well plates and genotyped. For genomic PCR for genotyping, the cells were digested by KAPA Express Extract (Nippon Genetics Co, Ltd., Tokyo, Japan) diluted in Tris-EDTA. Genomic PCR was performed using KOD FX Neo DNA polymerase (TOYOBO Co. Ltd., Osaka, Japan) with genotyping primers.

2.15 | PiggyBac transposon vector system

FOLR1 stably expressing cell lines were produced by introducing the pPB-CAG-FOLR1-IRES-Puro vector into MKN1 also used above. The FOLR1 cDNA obtained by KOD Plus NEO DNA polymerase was cloned into the EcoRI-digested site of the pPB-CAG-IRES-Puro plasmid to create the pPB-CAG-FOLR1-IRES-Puro vector. The pPB-CAG-FOLR1-IRES-Puro vector was electroporated into 1×10^6 MKN1 using a NEPA21 electroporation system (NEPA-GENE, Chiba, Japan) with a plasmid coding the piggyBac transposase (PBBase). The transfected cells were cultured in 10% FCS (Foetal Calf Serum)-DMEM supplemented with 10 ng/ml puromycin for 10 days.

2.16 | In vivo tumor growth assay

Gastric cancer cell lines (1×10^7 cells per mouse) were injected subcutaneously into the right flank of 6-week-old female BALB/cAJcl-nu/nu mice. After tumors had achieved a target volume of 100 to 200 mm³, mice were randomly assigned to treatment groups and received a single intraperitoneal injection of PBS (100 µL, control) or of MORAb-202 (5 mg/kg) or an equivalent molar dose of eribulin (0.1 mg/kg) (day0). The dose of MORAb-202 was based on the results of a previous in vivo study.⁶ The molecular masses of MORAb-202, eribulin mesylate, and farletuzumab are 155.2 kDa, 826.0 Da, and 29.8 kDa, respectively. Calculations were performed with a drug to antibody ratio for MORAb-202 of 4. Tumor volume was measured twice a week, and body weight was measured once or twice a week.

The antitumor effects of MORAb-202 versus PBS were demonstrated with the tumors that were excised from mice on day11, and tumor sections were prepared and fixed in formalin for subsequent experiments.

2.17 | Hematoxylin and eosin staining

Tumor sections (5 µm) were stained with hematoxylin for 10 min, differentiated with 1% hydrochloric acid, and stained with eosin solution for 30 s. The sections were mounted on glass slides for pathological observations.

2.18 | Survival analysis

An online tool (Kaplan-Meier plotter, <https://kmplot.com/analysis>) was used to assess the relation between FOLR1 mRNA abundance and overall survival for gastric cancer patients. The patients were divided into two groups based

on the expression level of *FOLR1*, with the cutoff being set automatically. The hazard ratio, its 95% confidence interval, and log-rank *P*-value were determined.

2.19 | Statistical analysis

One-way ANOVA followed by Tukey's honestly significant difference (HSD) test was performed with the use of GraphPad Prism 5 software. A *P*-value of $< .05$ was considered statistically significant.

2.20 | Additional methods

Additional methods are provided in Supporting Information Methods online.

3 | RESULTS

3.1 | FOLR α expression in gastric and other cancer types

We first performed immunohistochemical analysis of FOLR α expression in various human cancer types, with gastric cancer having been shown to be among the tumor types with the highest rates of FOLR α positivity, after ovarian, endometrial, lung, and breast cancers.⁴ Among 133 gastric cancer specimens, 8.3% (11/133) were weakly positive, and 13.5% (18/133) were strongly positive for FOLR α expression, yielding a total positive rate of 21.8% (Figure 1A). FOLR α -positive gastric tumors included all main histological subtypes (Table S1), and FOLR α staining was detected both at the cell membrane and in the cytoplasm (Figure 1B). We also examined the relationship between HER2 and FOLR α positivity in gastric cancer by tissue microarray analysis. The expression of FOLR α was more frequent among tumors positive for HER2 expression than among those negative [56.4% (22/39) versus 24.8% (25/101); $P < .001$, Pearson's Chi-squared test].

Although a meta-analysis previously showed that a high expression level of FOLR α is associated with poor survival in patients with ovarian, endometrial, lung, or breast cancer,⁷ the situation for patients with gastric cancer has been unclear. We, therefore, examined the possible impact of FOLR α expression on the survival of 875 gastric cancer patients in the Gene Expression Omnibus (GEO) database. Overall survival was significantly ($P < .001$) shorter for patients with a high level of *FOLR1* expression in their tumors than in those with a low level (Figure 1C), suggesting that FOLR α expression may be related to tumor aggressiveness in gastric cancer.

3.2 | FOLR α promotes the proliferation of gastric cancer cells

To understand the mechanism underlying the poor prognosis of gastric cancer expressing *FOLR1* at a high level, we examined the abundance of *FOLR1* mRNA and FOLR α protein in various human gastric cancer cell lines by RT-qPCR analysis and immunoblot analysis, respectively. We found that among eight such cell lines, MKN1, NCI-N87, and MKN74 showed relatively high levels of both *FOLR1* mRNA and FOLR α protein (Figure 2A). Immunofluorescence analysis revealed both membranous and cytoplasmic staining for FOLR α in MKN1 and MKN74 cells (Figure 2B and Supplementary Figure S1), consistent with our results for human gastric cancer specimens and supporting the validity of these cell lines for the study of FOLR α function in gastric cancer.

We next examined the effects of knockdown of *FOLR1* mRNA in MKN1 and MKN74 cells by RNA interference. The knockdown efficiency for the *FOLR1*-targeting siRNA (siFOLR1) was found to be 78% by RT-qPCR analysis in MKN1 cells compared to control transfected with scrambled RNA (scrambled control) (Figure 2C). Transfection with siFOLR1 attenuated cell proliferation without inducing cell death in both MKN1 and MKN74 cells, although the antiproliferative effect in the latter cells did not achieve statistical significance (Figures 2D and 2E). Together, these data suggested that FOLR α is required for the proliferation but not the survival of gastric cancer cells.

3.3 | Relation of FOLR α expression to low apoptotic activity in gastric cancer

To investigate the molecular pathways in which FOLR α functions, we performed RNA-sequencing (RNA-seq) analysis for tumors formed by MKN1 cells in nude mice (Figure S2A). The isolated tumor cells were first subjected to fluorescence-activated cell sorting (FACS) to obtain two populations expressing FOLR α at a high or low level. Gene ontology (GO) analysis revealed 18 genes related to "extracellular matrix organization," 19 genes related to "extracellular structure organization," 11 genes related to "regulation of extrinsic apoptotic signaling pathway," 6 genes related to "regulation of cell adhesion mediated by integrin," 11 genes related to "cell-matrix adhesion," or 6 genes related to "cell adhesion mediated by integrin" were upregulated in the FOLR α -high population while 14 genes related "positive regulation of leukocyte proliferation," 9 genes related to "regulation of protein activation cascade," 13 genes related to "positive regulation of lymphocyte proliferation" were downregulated (Figure S2B).

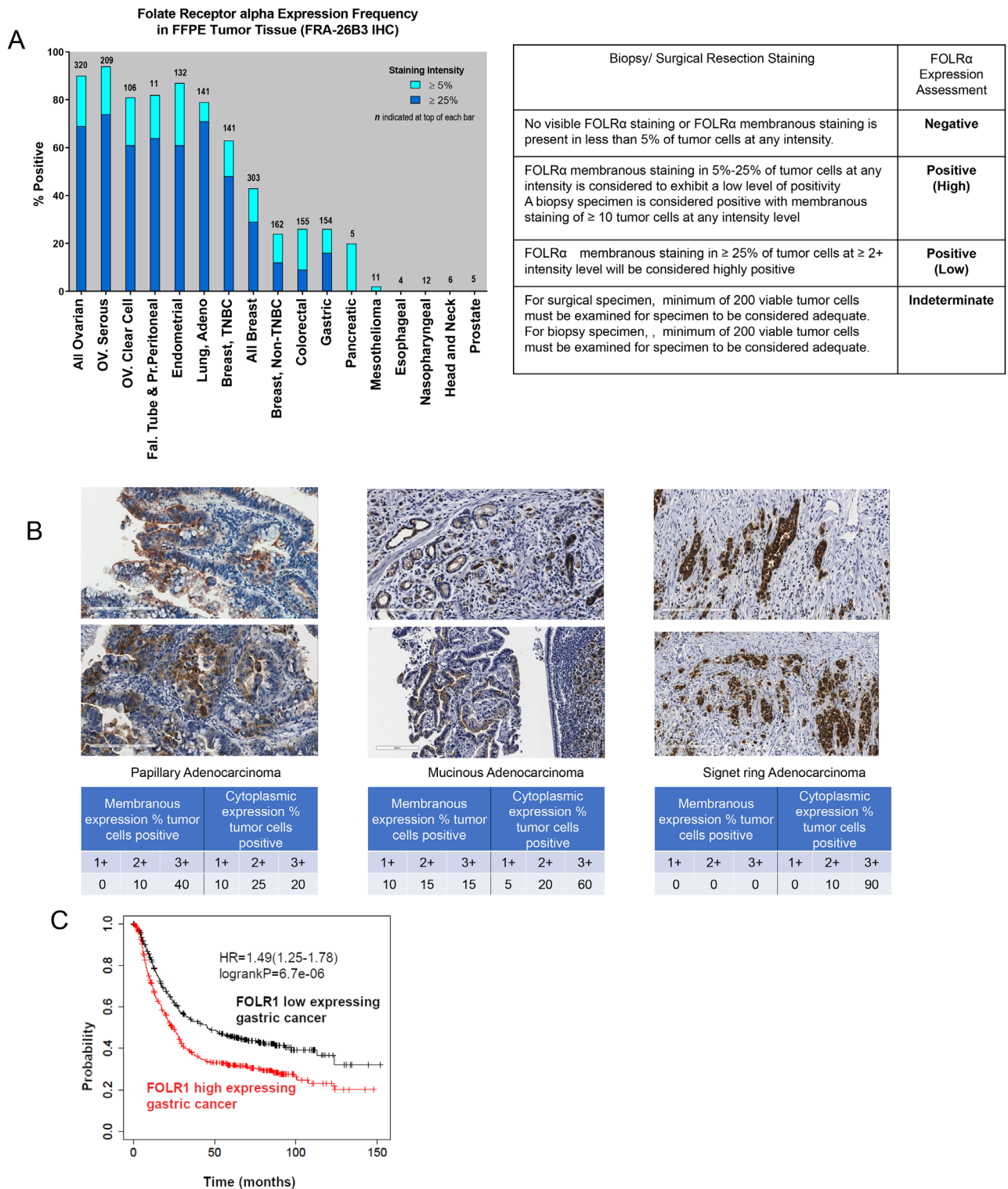


FIGURE 1 FOLRα expression in human gastric cancer. A, Frequency of FOLRα protein expression in various human cancer types. The percentage of tumors of each type positive for FOLRα expression was determined by immunohistochemistry. Dark and light blue shading correspond to tumors classified as strongly or weakly positive for FOLRα staining, as described in Supplementary Methods. The number at the top of each bar indicates the number of positive tumors. OV. Seous, ovarian serous carcinoma; OV. Clear Cell, ovarian clear cell carcinoma; Fal. tube & Pr.peritoneal, fallopian tube and primary peritoneal cancer; adeno, adenocarcinoma; TNBC, triple-negative breast cancer. The table indicates scoring criteria for FOLRα immunohistochemical staining. B, Representative immunohistochemistry images of FOLRα staining in gastric cancer specimens. The percentages of tumor cells positive for membranous or cytoplasmic staining at each intensity level are shown below each image. Scale bars, 200 μm. C, Kaplan-Meier curves of overall survival according to FOLR1 expression level for 875 gastric cancer patients in the GEO database. The curves were generated with the use of Kaplan-Meier plotter (<http://kmplot.com/analysis>). The hazard ratio (HR) with its 95% confidence interval as well as the log-rank P value is shown

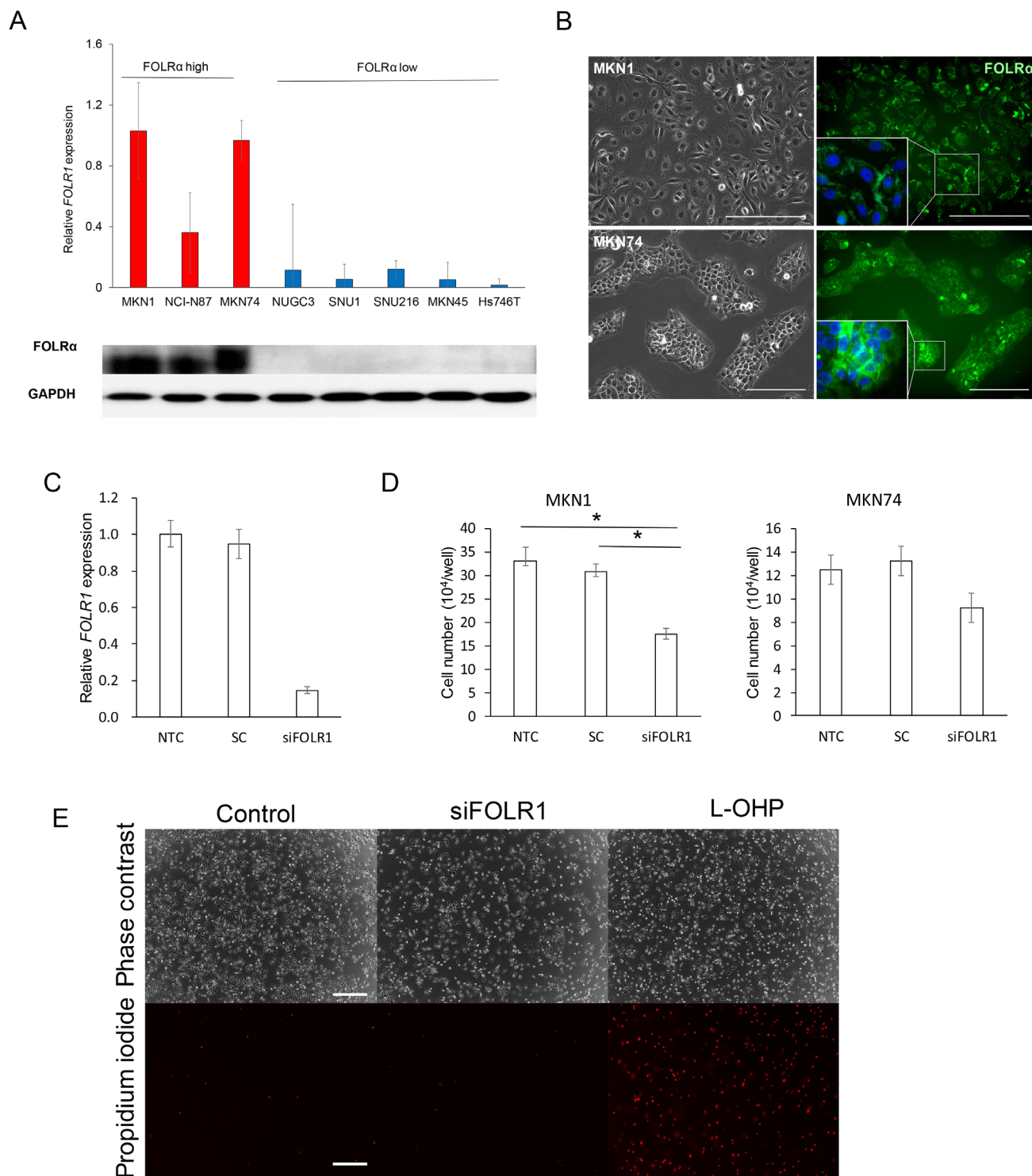


FIGURE 2 FOLR α expression and function in human gastric cancer cell lines. **A**, RT-qPCR analysis of *FOLR1* mRNA and immunoblot analysis of FOLR α protein in eight gastric cancer cell lines. The RT-qPCR data are means \pm SD from four independent experiments. Glyceraldehyde-3-phosphate dehydrogenase (GAPDH) was examined as a loading control for immunoblot analysis. **B**, Immunofluorescence staining of FOLR α (green) in MKN1 and MKN74 cells (right). Nuclei were stained with 4',6-diamidino-2-phenylindole (DAPI, blue). Phase-contrast images are also shown (left). Scale bars, 500 μ m. **C**, RT-qPCR analysis of *FOLR1* mRNA in MKN1 cells transfected (or not, NTC) with siFOLR1 or a scrambled control siRNA (SC). Data are means \pm SD for four independent experiments. **D**, Cell number for MKN1 or MKN74 cells transfected as in **C**, plated at a density of 5×10^4 cells per well, and then cultured for 24 h. Data are means \pm SD for four independent experiments. * $P < .05$ (one-way ANOVA followed by Tukey's post hoc test). **E**, Viability of MKN1 cells treated as in **D**. Dead cells were detected by fluorescence microscopy after staining with propidium iodide. Phase-contrast images are also shown. MKN1 cells treated with 5 μ g/ml oxaliplatin (L-OHP) for 48 h were examined as a positive control for induction of cell death. Scale bars, 500 μ m

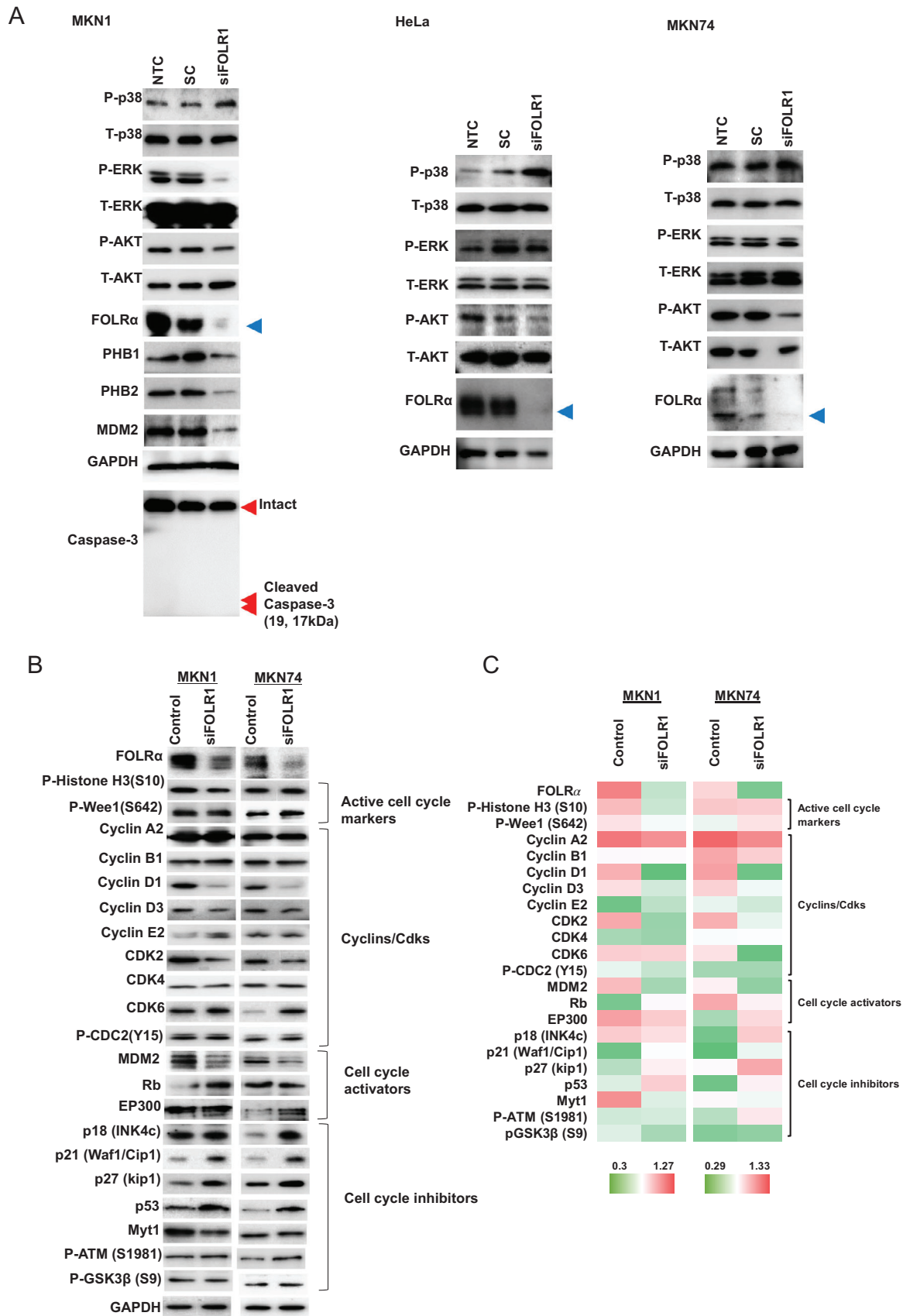


FIGURE 3 Screening of molecules that contribute to the phenotype of FOLRα-expressing gastric cancer. A, Immunoblot analysis of the effects of FOLRα depletion on MAPK and AKT signaling in MKN1, HeLa, and MKN74 cells. Cells transfected (or not, NTC) with siFOLR1 or a scrambled control siRNA (SC) were subjected to immunoblot analysis with antibodies to the indicated proteins. Phosphorylated (P) and total

We next performed a microarray analysis of control and FOLR α -depleted MKN1 cells and examined the differential expression of genes related to cell proliferation, cell survival, or metastasis with the use of WikiPathways (Figure S3). Among genes related to “apoptosis,” the expression of *MDM2* was down-regulated, whereas that of *APAF1*, *TNFSF10*, *CASP1*, *CASP6*, *CASP7*, and *PMAIP1* was up-regulated in the FOLR α -depleted cells. The expression of substantial numbers of genes related to “cell cycle,” “focal adhesion,” “TGF-beta receptor signaling pathway,” or “Wnt signaling” was also downregulated by FOLR α knockdown.

Together, these findings suggested that FOLR α is positively associated with cell proliferation and negatively associated with extracellular matrix organization/adhesion and apoptosis. Given that knockdown of FOLR α suppressed cell proliferation without affecting cell viability in gastric cancer cell lines (Figure 2C–E); however, the up-regulation of apoptosis-related gene expression in cells depleted of FOLR α appears to be insufficient to trigger apoptosis.

3.4 | Knockdown of FOLR α induces downregulation of MDM2

We performed immunoblot analysis to examine the possible effects of FOLR α depletion on signaling by the mitogen-activated protein kinases (MAPKs), ERK (extracellular signal-regulated kinase), and p38 as well as by the protein kinase AKT (Figure 3A). However, we obtained inconsistent results for the effects of FOLR α knockdown on the phosphorylation of these proteins in MKN1 cells, MKN7 cells, and HeLa cells (a human cervical cancer cell line known to express FOLR α at a high level). To identify proteins that might interact with FOLR α and thereby contribute to the regulation of cell proliferation, we compared the scrambled control and FOLR α -depleted MKN1 or MKN7 cells for the expression of proteins related to the cell cycle or cell survival, including active cell cycle markers (phospho-histone H3 and phospho-Wee1), cyclins and cyclin-dependent kinases (cyclins A2, B1, D1, D3, and E2; CDK2, CDK4, CDK6, and phospho-CDC2), cell cycle activators (MDM2, Rb, and EP300), and cell cycle

inhibitors [p18(Ink4c), p21(Waf1/Cip1), p27(Kip1), p53, Myt1, phospho-ATM, and phospho-GSK3 β] (Figures 3B and 3C). Immunoblot analysis revealed that knockdown of FOLR α resulted in down-regulation of cyclin D1, cyclin D3, CDK2, and MDM2 as well as in up-regulation of p21(Waf1/Cip1), p27(Kip1), and p53 in both MKN1 and MKN74 cells (Figures 3B and 3C). Among these proteins, the ubiquitin ligase MDM2 serves as a hub that interacts with multiple proteins related to cell proliferation, cell cycle, or gene transcription.^{8,9}

3.5 | PHB2 is a mediator of FOLR α -MDM2 interaction

We next investigated the functional relation between FOLR α and MDM2. Given that physical interaction between FOLR α and MDM2 was not detected by co-immunoprecipitation analysis (Figure 4A), we hypothesized that another protein might mediate any such interaction between FOLR α and MDM2. To identify such a protein, we performed liquid chromatography and tandem mass spectrometry (LC-MS/MS) of FOLR α immunoprecipitates prepared from HeLa cells (Figure 4B and Table S2). HeLa cells were used as a substitute for MKN1 cells in LC-MS/MS analysis, given that the relative abundance of *FOLR1* mRNA in the former cells was 1.27 ± 0.32 compared with 1.03 ± 0.26 for the latter. Again, physical interaction between FOLR α and MDM2 was not detected. Among the proteins found to bind to FOLR α , we focused on those whose function is related to cell proliferation or survival and localized to the cytoplasm or cell membrane and may come into contact with FOLR α . Among such proteins identified by the LC-MS/MS analysis, PHB2 was known to interact with MDM2 directly.¹⁰ We therefore further examined PHB2 and the related protein prohibitin1 (PHB1), both of which localize to mitochondria, the nucleus, and the cell membrane and contribute to the regulation of cell proliferation, apoptosis, and metastasis.¹¹ Co-immunoprecipitation analysis of MKN1 cells suggested that FOLR α might bind preferentially to PHB2 rather than to PHB1 (Figure 4C and Supplementary Figure S5). To examine whether PHB2 might mediate the interaction between FOLR α and MDM2, we performed

(T) forms of proteins were examined, with GAPDH serving as a loading control. The blue arrowheads indicate the FOLR α bands. B, Immunoblot analysis of the effects of FOLR α knockdown on the expression of proteins related to the cell cycle or cell survival in MKN1 and MKN74 cells. MKN1 or MKN7 cells were transfected with siFOLR1 or a scrambled control siRNA. Phosphorylated residues are indicated for phosphorylated proteins. C, Heat map for the expression of proteins related to the cell cycle or cell survival in MKN1 or MKN7 cells transfected with siFOLR1 or a scrambled control siRNA. The results were derived by quantifying the immunoblot data shown in Figure 3B using ImageJ (NIH) software and GAPDH as a calibration control. Red and green correspond to high and low relative protein expression levels, respectively, in each cell line

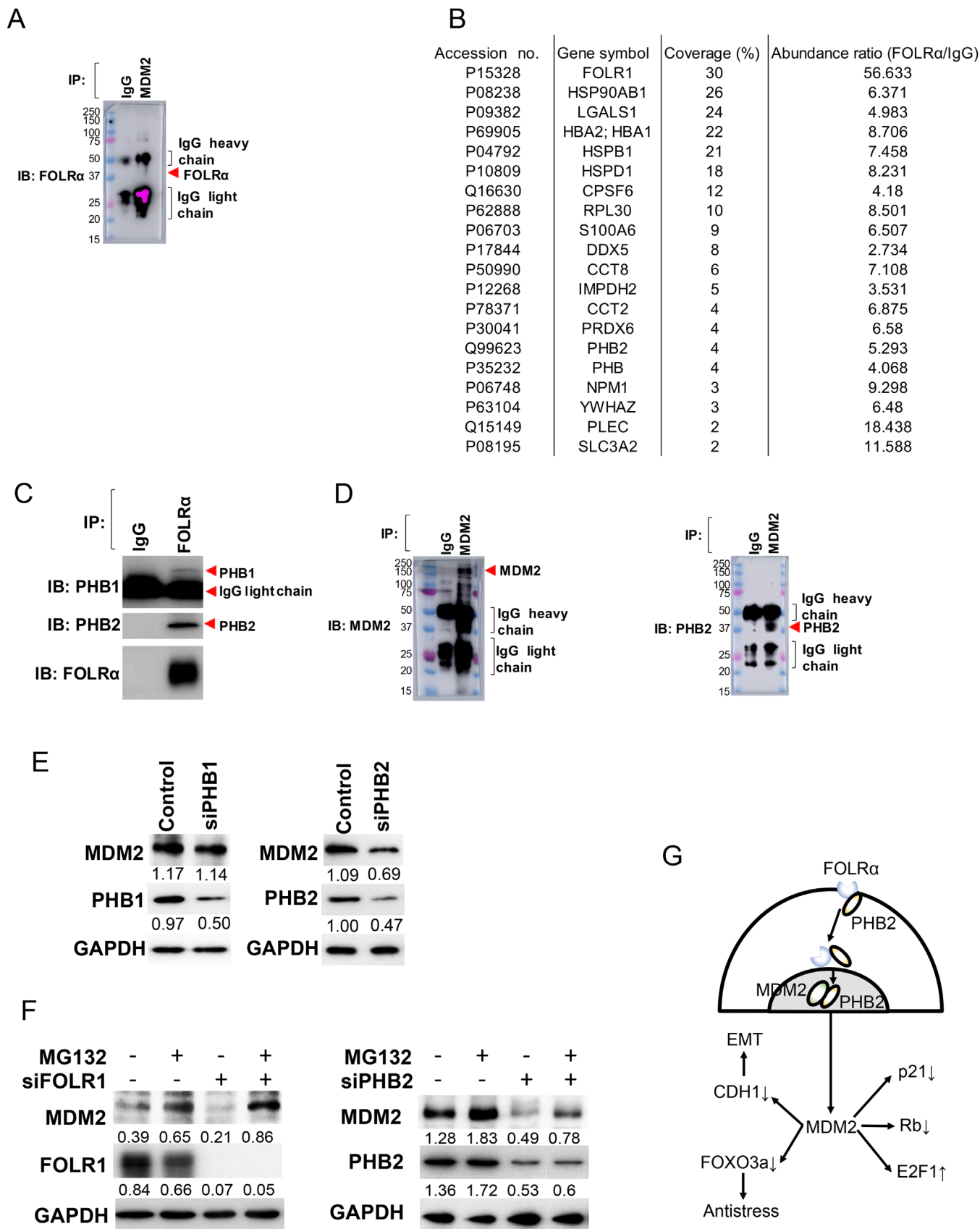


FIGURE 4 Identification of a FOLR α -PHB2-MDM2 axis in gastric cancer cells. **A**, IB analysis of FOLR α in MDM2 immunoprecipitates prepared from MKN1 cells. Molecular size markers (kilodaltons) are shown in the leftmost lanes. **B**, Binding partners of FOLR α identified by LC-MS/MS analysis of FOLR α immunoprecipitates prepared from HeLa cells. Among 206 such proteins identified, the 19 proteins shown in addition to FOLR α were chosen on the basis of their function and intracellular distribution. **C**, Immunoblot (IB) analysis of PHB1, PHB2, and

immunoblot analysis of MDM2 immunoprecipitates prepared from MKN1 cells (Figure 4D). Whereas FOLR α was not detected in association with MDM2, PHB2 was clearly detected in the MDM2 immunoprecipitates.

We next investigated the possible effect of PHB1 or PHB2 on MDM2 expression (Figure 4E and Supplementary Figure S5). Transfection of MKN1 cells with a siRNA specific for PHB2 (siPHB2) achieved a knockdown efficiency of 53% resulted in a 37% decrease in the amount of MDM2, whereas the abundance of MDM2 was largely unchanged after transfection with a PHB1 siRNA (siPHB1), suggesting the possibility that interaction between FOLR α and PHB2 might stabilize MDM2. To determine whether FOLR α and PHB2 affect the proteasome-mediated degradation of MDM2, we transfected MKN1 cells with siFOLR1 or siPHB2 and then exposed the transfected cells to the proteasome inhibitor MG132 (Figure 4F and Figure S5). Immunoblot analysis revealed that FOLR α or PHB2 knockdown efficiency was 89% to 94% and 56% to 69%, respectively. Whereas transfection with siFOLR1 or siPHB2 resulted in the downregulation of MDM2, MG132 increased the abundance of MDM2 both in control and in FOLR α - or PHB2-depleted cells, suggesting that the proteasomal degradation of MDM2 is balanced by FOLR α -PHB2. Given that MDM2 is implicated in epithelial-mesenchymal transition (EMT),¹² in degradation of the transcription factor FOXO3a,¹³ the CDK inhibitor p21(Waf1/Cip1),¹⁴ and the tumor suppressor Rb,¹⁵ as well as in the stabilization of the transcription factor E2F1,¹⁶ our results suggest that MDM2 might determine the malignant phenotype of FOLR α -expressing cancer as a result of the operation of a FOLR α -PHB2-MDM2 axis (Figure 4G).

3.6 | Promotion of chemotherapeutic efficacy by knockdown of FOLR α but not by farletuzumab

Given that MDM2 is also implicated in resistance to chemotherapy,^{17,18} we examined whether the FOLR α -

PHB2-MDM2 axis might confer such resistance. We found that transfection with siFOLR1 or siMDM2 significantly inhibited the proliferation of MKN1 cells exposed to oxaliplatin (5 or 50 μ g/ml), a platinum agent administered for the treatment of gastric cancer (Figures 5A and 5B). Knockdown of FOLR α thus enhanced the sensitivity of gastric cancer cells to cytotoxic chemotherapy to a similar extent as did that of MDM2.

We next examined the anticancer efficacy of the humanized anti-FOLR α mAb farletuzumab.¹⁹ The addition of farletuzumab (1, 3, or 10 μ g/ml) to 2 nM (1.5 ng/ml) eribulin, an anti-microtubule agent, or to 13 μ M (5 μ g/ml) oxaliplatin had no additional antiproliferative effect on MKN1 cells (Figure 5C), suggestive of the limited efficacy of the addition of farletuzumab to cytotoxic agents for the treatment of gastric cancer.

3.7 | The efficacy of MORAb-202 depends on the expression level of FOLR α both in vitro and in vivo

We next examined the effects of a newly developed ADC, MORAb-202, consisting of farletuzumab conjugated to eribulin. We first tested the antiproliferative activity of MORAb-202 in human gastric cancer cell lines with various levels of FOLR α expression in vitro (Figure 5D). MORAb-202 inhibited cell proliferation more efficiently in cell lines with a high level of FOLR α expression—including MKN1, MKN74, and NCI-N87—than in those with a low level of FOLR α expression, including MKN45, NUGC3, and SNU216.

To confirm whether FOLR α expression indeed determines the antiproliferative activity of MORAb-202 in vitro, we performed a cell proliferation assay with MKN1 cells in which both alleles of the endogenous *FOLR1* gene had been disrupted with the use of the CRISPR/Cas9 system (Figure S4). Indeed, we found that the efficacy of MORAb-202 was increased in the cells overexpressing FOLR α and was attenuated in those lacking FOLR α compared with parental MKN1 cells (Figure 5E).

FOLR α in immunoprecipitates (IP) prepared from MKN1 cells with antibodies to FOLR α or control immunoglobulin G (IgG). D, IB analysis of MDM2 and PHB2 in MDM2 immunoprecipitates prepared from MKN1 cells. {Molecular size markers (kilodaltons) are shown in the leftmost lanes. E, IB analysis of MDM2, PHB1, and PHB2 in MKN1 cells transfected with siPHB1, siPHB2, or a scrambled control siRNA as indicated. Band intensity was quantified with the use of ImageJ (NIH) software and with GAPDH as a calibration control. Results are representative of three independent experiments. F, Immunoblot analysis of MDM2, FOLR α , and PHB2 in MKN1 cells transfected with siFOLR1 or siPHB2, as indicated, and then incubated in the absence or presence of MG132 at 1 nM for 6 h. Band intensity was quantified with the use of ImageJ (NIH) software and with GAPDH as a calibration control. Results are representative of three independent experiments. G, Model for the operation of a FOLR α -PHB2-MDM2 axis in gastric cancer. PHB2 mediates the interaction between FOLR α and MDM2 and thereby regulates p53-dependent or -independent functions of MDM2, including promotion of EMT, degradation of FOXO3a, p21(Waf1/Cip1), and Rb, as well as stabilization of E2F1

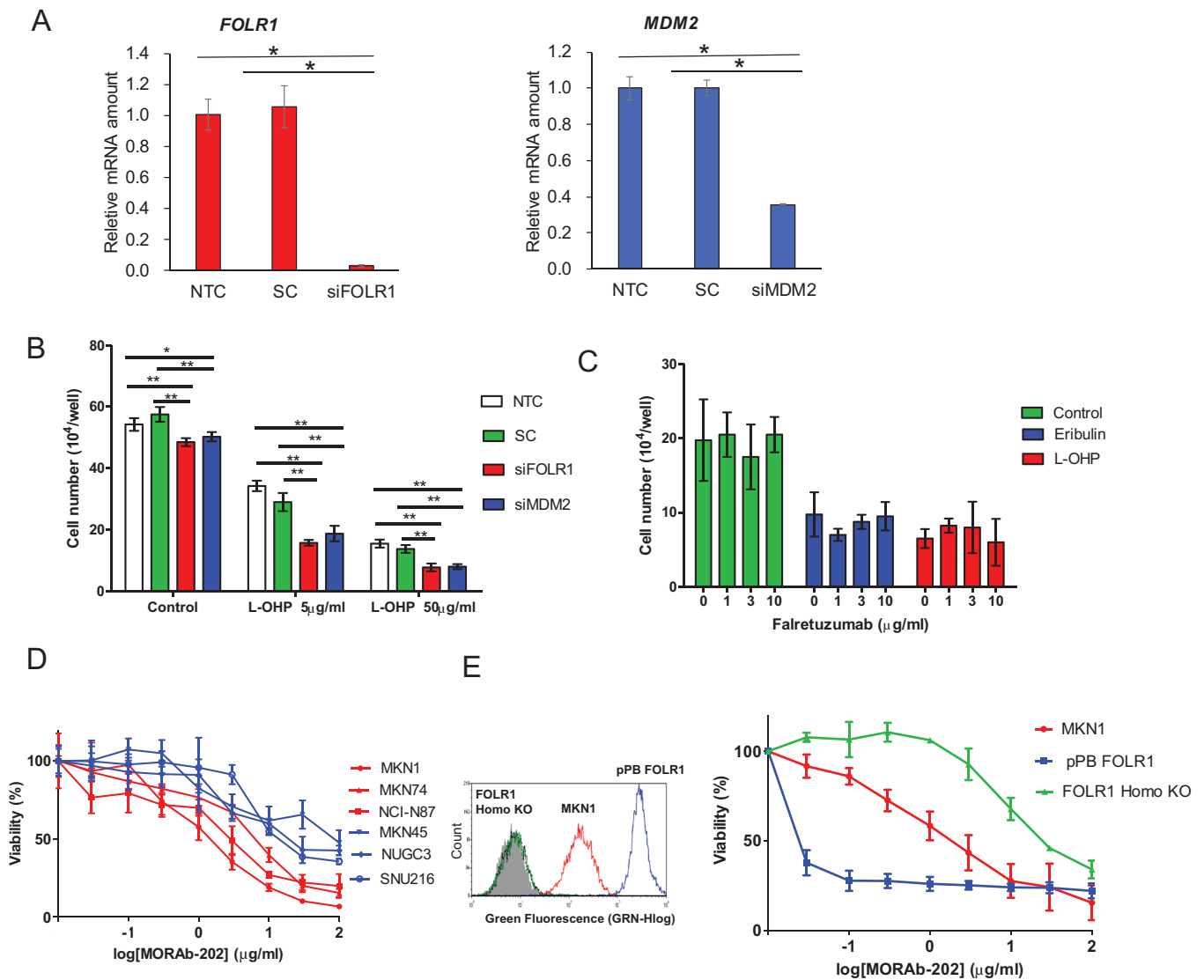


FIGURE 5 Antitumor efficacy of MORAb-202 for FOLR α -positive gastric cancer. **A**, RT-qPCR analysis of *FOLR1* and *MDM2* mRNA abundance in MKN1 cells transfected with siFOLR1 or siMDM2, respectively. Nontransfected cells (NTC) and cells transfected with a scrambled siRNA (SC) were also examined as controls. Data are means \pm SD from four independent experiments. * $P < .05$ (one-way ANOVA and Tukey's post hoc test). **B**, Cell number for MKN1 cells transfected as in **A**, plated at a density of 5×10^4 cells per well, and then cultured for 24 h in the absence or presence of oxaliplatin (L-OHP, 5 or 50 μ g/ml). Data are means \pm SD for four independent experiments. * $P < .05$, ** $P < .01$ (one-way ANOVA followed by Tukey's post hoc test). **C**, Cell number for MKN1 cells plated at a density of 5×10^4 cells per well, exposed to the indicated concentrations of faltretuzumab for 24 h, and then incubated in the additional absence or presence of eribulin (1.5 ng/ml) or oxaliplatin (5 μ g/ml) for 24 h. Data are means \pm SD from four independent experiments. **D**, Cell proliferation assay for gastric cancer cell lines treated with various concentrations of MORAb-202 (0.01–100 μ g/ml) for 120 h. Cell lines expressing FOLR α at a high or low level are shown in red and blue, respectively. Data are means \pm SD from six independent experiments. **E**, MKN1 cells transfected with an expression vector for human FOLR α (pPB-FOLR1) or rendered homozygous for a disrupted *FOLR1* allele with the use of the CRISPR/Cas9 system (FOLR1 Homo-KO) were assayed for cell surface expression of FOLR α by flow cytometry (left panel) or were incubated with various concentrations of MORAb-202 for 120 h and then assayed for cell viability (right panel). Viability data are means \pm SD from three independent experiments

Finally, we compared the antitumor activity of MORAb-202 and an equivalent molar dose of eribulin in nude mice harboring tumors formed by gastric cancer cell lines expressing FOLR α at a high (MKN1, NCI-N87) or low (NUGC3) level. Consistent with previous findings,⁶

MORAb-202 had a marked and prolonged inhibitory effect on the growth of tumors formed by MKN1 or NCI-N87 cells (Figure 6A–C). MORAb-202 at a dose of 5 mg/kg showed a significantly ($P < .05$) higher antitumor efficacy than did the equivalent molar dose of eribulin in MKN1 cells

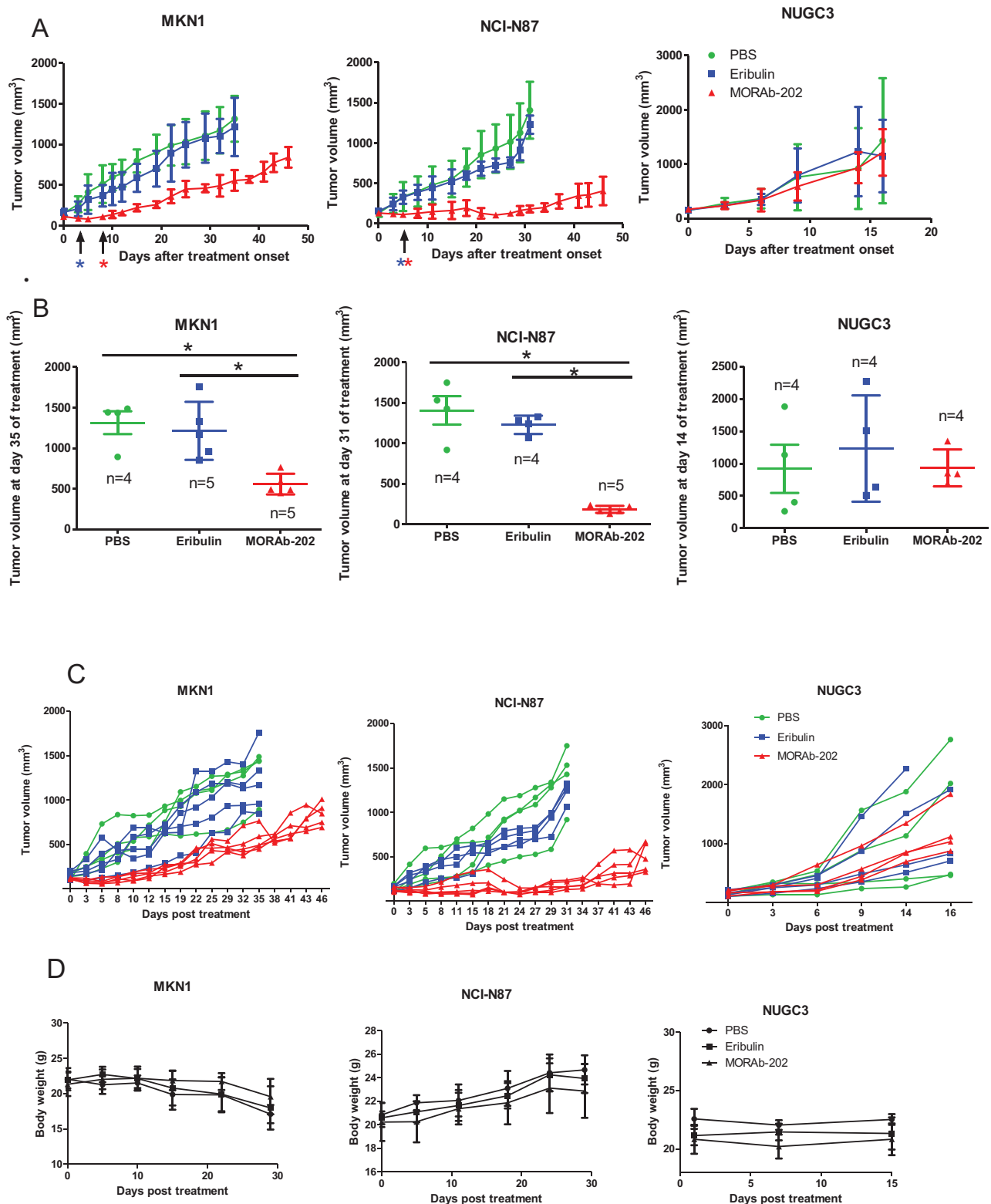


FIGURE 6 The effect of MORAb-202 on the xenograft with high FOLR α expression and those with FOLR α low expression. **A**, Tumor volume for nude mice bearing subcutaneous tumors formed by MKN1, NCI-N87, or NUGC3 cells and treated intraperitoneally with MORAb-202 (5 mg/kg), the equivalent molar dose of eribulin (0.1 mg/kg), or PBS vehicle (100 μ l) on day 0. Data are means \pm SEM. Red and blue asterisks indicate $P < .05$ for comparisons between MORAb-202 and eribulin and between MORAb-202 and PBS at the indicated times, respectively (one-way ANOVA followed by Tukey's post hoc test). **B**, Tumor volume determined as in (A) for MKN1 cells at day 35, NCI-N87 cells at day 31, and NUGC3 cells at day 14. Individual values and the mean \pm SEM are shown. $*P < .05$. **C**, Tumor volume for each mouse treated with MORAb-202, eribulin, or PBS in Figure 6A. **D**, The body weight of mice treated with MORAb-202, eribulin, or PBS in Figure 6A. Data in D are means \pm SEM

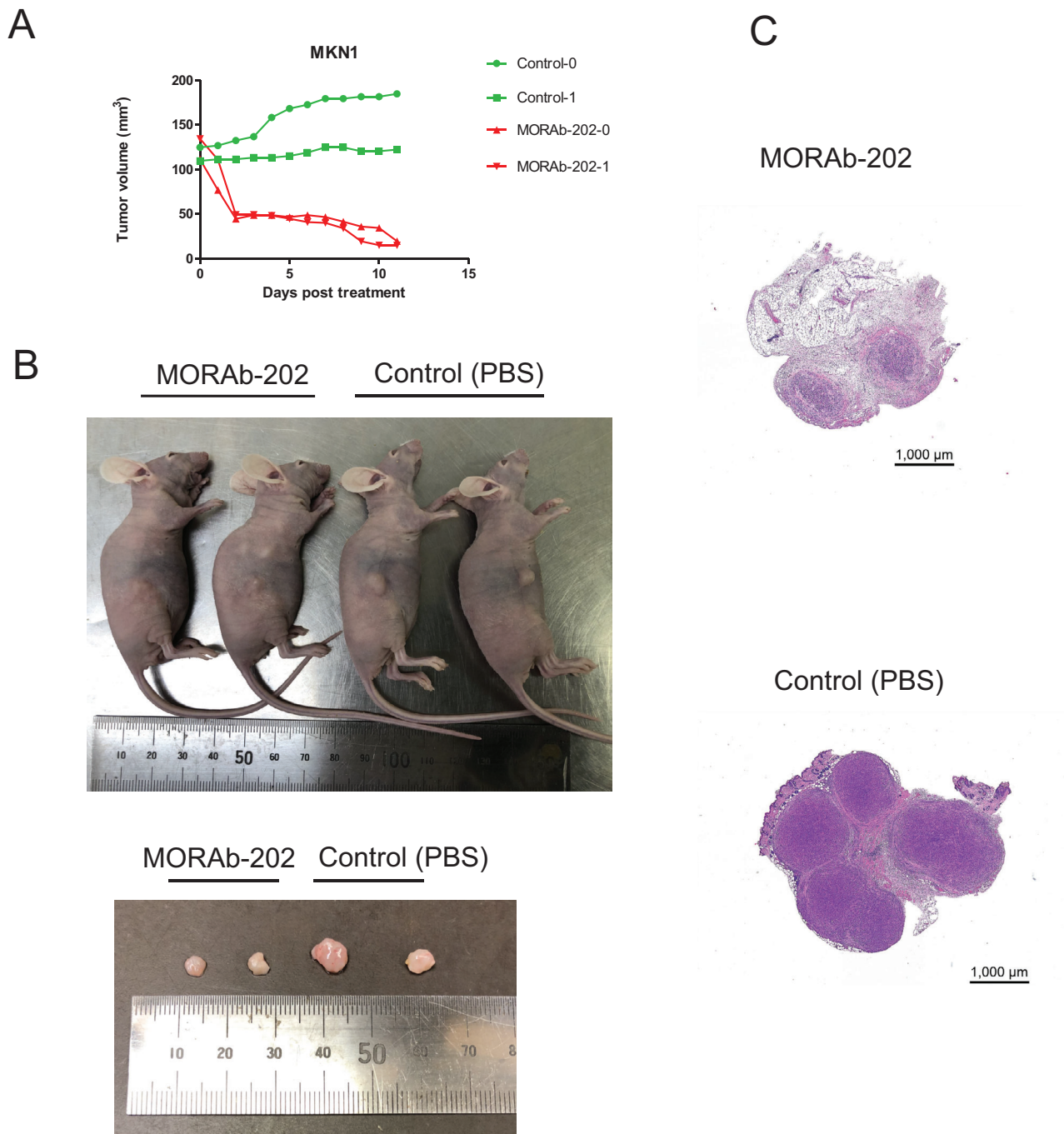


FIGURE 7 Inhibition of tumor growth by MORAb-202 in nude mice xenografted with MKN1. A, Tumor volume of each mouse treated with MORAb-202 or PBS. B, Photographs of mice and dissected tumors on day11. C, Representative images of hematoxylin and eosin-stained sections of tumors from mice treated with MORAb-202 and mice treated with PBS (Control)

from day 8 and in NCI-N87 cells from day 5. MORAb-202 at this dose had no effect on body weight in the treated mice (Figure 6D). In contrast, MORAb-202 did not affect the growth of NUGC3 xenografts (Figure 6A–C). Antitumor activity of MORAb-202 was observed on day 11 (Figure 7A–C). Together, our results revealed target-specific antitumor activity of MORAb-202 for gastric cancer cells expressing FOLR α at a high level.

4 | DISCUSSION

We found that FOLR α is expressed in various histological subtypes of gastric cancer, with this expression being more frequent in HER2-positive cases than in HER2-negative ones, as previously shown for *EGFR* mutation-positive lung adenocarcinoma,²⁰ suggestive of an association between FOLR α expression and an aggressive

phenotype of cancer. RNA-seq analysis of FOLR α -high and FOLR α -low fractions revealed lower levels of expression of apoptosis-related genes and higher levels of protein activation cascade- and proliferation-related genes in the FOLR α -high cells and downregulation of FOLR α affected cell proliferation. Furthermore, ablation of the *FOLR1* gene by CRISPR/Cas9 technology did not seem to affect MKN1 cell survival. These results thus indicate that FOLR α is not essential for the survival of gastric cancer cells but contributes to the regulation of cell proliferation under basal conditions.

We found that FOLR α was localized not only at the cell membrane and but also in the cytoplasm both of gastric cancer cells in human tumor specimens and of MKN1 and MKN74 cell lines, suggesting that FOLR α might interact with cytoplasmic proteins such as protein kinases. Although FOLR α was previously shown to contribute to the regulation of the ERK signaling pathway,⁴ we did not detect consistent effects of FOLR α knockdown on signaling by ERK, p38 MAPK, or AKT, suggesting that the interaction between FOLR α and ERK may be dependent on cell type or context. To identify molecules that contribute to the phenotype of FOLR α -expressing gastric cancer, we performed immunoblot and microarray analyses focusing on molecules related to cell proliferation or survival, and we found that knockdown of FOLR α resulted in downregulation of MDM2 expression.

MDM2 is a key player in regulating cell proliferation, TGF- β signaling,²¹ cell adhesion and invasion, and EMT,¹² and it contributes to chemotherapy resistance.^{17,18} It was, therefore, a candidate mediator of the link between FOLR α expression and malignancy of gastric cancer. However, the co-immunoprecipitation analysis did not detect a substantial physical association between FOLR α and MDM2, suggesting that another molecule might be required to mediate the interaction between these two proteins. We performed LC-MS/MS analysis of FOLR α immunoprecipitates to identify such a molecule. We focused on PHB1 and PHB2, which together function as a chaperone and stabilize various proteins in mitochondria.^{11,22} We found that PHB2 bound to MDM2 in a co-immunoprecipitation assay, consistent with the previous finding that PHB2 can bind to MDM2 through its p53 BOX-I binding site,¹⁰ and that knockdown of PHB2 resulted in downregulation of MDM2 expression. On the basis of these findings, we concluded that FOLR α interacts with MDM2 via PHB2 and that such interaction mediates the stabilization of MDM2. Thus, our results identified the operation of a FOLR α -PHB2-MDM2 axis in gastric cancer cells, and they further implicated this axis in chemotherapy resistance.

We thus found that knockdown of FOLR α , as well as that of MDM2, significantly increased the sensitivity of MKN1 cells to oxaliplatin in vitro. We, therefore, exam-

ined the effect of farletuzumab, a humanized mAb to FOLR α that has shown antitumor efficacy in a preclinical model of ovarian cancer.^{19,23} In MKN1 cells, however, farletuzumab did not show antitumor efficacy either as monotherapy or in combination with oxaliplatin or eribulin. This difference between the effects of FOLR α knockdown and farletuzumab may be attributable to the fact that the mAb simply binds to the extracellular domain of FOLR α , and it might therefore not affect the operation of the FOLR α -PHB2-MDM2 axis in the cytoplasm. Thus our results suggest that targeting of FOLR α alone by farletuzumab may not be sufficient to downregulate MDM2 function in gastric cancer and that the therapeutic efficacy of farletuzumab, even in combination with chemotherapy, may be limited.

We next evaluated the efficacy of MORAb-202, a farletuzumab-eribulin ADC that is currently under clinical investigation in gastric cancer cell lines. Consistent with previous findings in other tumor types,⁶ we found that the antitumor efficacy of MORAb-202 for gastric cancer cell lines in vitro and in vivo was dependent on the level of FOLR α expression and that that for tumors formed by FOLR α -high cell lines in vivo was greater than the efficacy of an equivalent dose of eribulin. Our results thus provide a rationale for the therapeutic targeting of FOLR α -positive gastric cancer with MORAb-202.

A limitation of the present study is that we evaluated only MORAb-202 as a FOLR α -targeted ADC and eribulin as a payload. Given that eribulin has been shown to suppress EMT,²⁴ it is expected to be effective against cancers with a phenotype characterized by down-regulation of the expression of genes related to cell-cell or cell-matrix adhesion. A clinical trial of MORAb-202 in patients with FOLR α -positive solid cancers is ongoing and has revealed encouraging antitumor activity (NCT03386942). Support for the treatment of FOLR α -positive tumors with a FOLR α -targeted ADC would be provided by elucidating the underlying mechanism of action. Here we provide a rationale for patient selection for treatment with MORAb-202 on the basis of immunohistochemical determination of FOLR α expression in a tumor specimen. Given the substantial prevalence of FOLR α expression in gastric cancer, our data support the clinical development of MORAb-202 for this tumor type.

ACKNOWLEDGMENTS

We thank Haruka Yamaguchi, Yume Shinkai, Michiko Kitano and Kanae Shigi for assistance. This study was funded by Eisai Incorporated.

AUTHOR CONTRIBUTIONS

Hitomi Sakai was associated with conceptualization, methodology, data acquisition, data analysis, and writing

the original draft. Hisato Kawakami was associated with conceptualization, methodology, data acquisition, data analysis, and revision of the manuscript. Takeshi Teramura was associated with conceptualization, methodology, data acquisition, data analysis, and revision of the manuscript. Yuta Onodera was associated with methodology, data acquisition, and data analysis. Elizabeth Somers was associated with methodology, data acquisition, and revision of the manuscript. Keiji Furuuchi was associated with data acquisition and material support. Toshimitsu Uenaka was associated with data acquisition and material support. Ryoji Kato was associated with methodology, data analysis, and revision of the manuscript. Kazuhiko Nakagawa was associated with conceptualization and study supervision. All the authors have final approval of the submitted paper.

ETHICS APPROVAL AND CONSENT TO PARTICIPATE

All animal experiments were approved by the Animal Ethics Committee of Kindai University.

CONSENT FOR PUBLICATION

This manuscript has been read and approved by all the authors to publish and is not submitted or under consideration for publication elsewhere.

CONFLICT OF INTEREST


HS has received research funding from Eisai Co. Ltd and Chugai Pharmaceutical Co. Ltd. HK has received consulting fees from Bristol-Myers Squibb Co. Ltd., Eli Lilly Japan K.K., MSD K.K., Ono Pharmaceutical Co. Ltd., Daiichi-Sankyo Co. Ltd., and Taiho Pharmaceutical Co. Ltd; honoraria from Bristol-Myers Squibb Co. Ltd., AstraZeneca K.K., Bayer yakuhin Ltd., Eli Lilly Japan K.K., MSD K.K., Ono Pharmaceutical Co. Ltd., Chugai Pharmaceutical Co. Ltd., Daiichi-Sankyo Co. Ltd., Takeda Pharmaceutical Co. Ltd., and Taiho Pharmaceutical Co. Ltd.; lecture fees from Bristol-Myers Squibb Co. Ltd., Eli Lilly Japan K.K., MSD K.K., Ono Pharmaceutical Co. Ltd., Chugai Pharmaceutical Co. Ltd., Takeda Pharmaceutical Co. Ltd., and Taiho Pharmaceutical Co. Ltd.; and research funding from Chugai Pharmaceutical Co. Ltd., Taiho Pharmaceutical Co. Ltd, and Eisai Co. Ltd. KN has received grants and personal fees from AstraZeneca K.K., grants and personal fees from Astellas Pharma Inc., grants and personal fees from MSD K.K., grants, personal fees and other from Ono Pharmaceutical Co.,Ltd., grants and personal fees from Nippon Boehringer Ingelheim Co.,Ltd., grants and personal fees from Novartis Pharma K.K., grants, personal fees and other from Pfizer Japan Inc., grants and personal fees from Bristol Myers Squibb Company, grants, personal fees and other from Eli Lilly Japan K.K., grants and personal fees from Chugai Pharmaceutical Co.,Ltd., grants and personal

fees from Daiichi Sankyo Co., Ltd., grants and personal fees from Merck Serono Co., Ltd./ Merck Biopharma Co., Ltd., during the conduct of the study; personal fees from Clinical Trial Co., Ltd., personal fees from MEDICUS SHUPAN, Publishers Co., Ltd., personal fees from Care Net, Inc, personal fees from Reno. Medical K.K., personal fees and other from KYORIN Pharmaceutical Co.,Ltd., personal fees from Medical Review Co., Ltd., personal fees from Roche Diagnostics K.K., personal fees from Bayer Yakuhin, Ltd, personal fees from Medical Mobile Communications co., Ltd, personal fees from 3H Clinical Trial Inc., personal fees from Nichi-Iko Pharmaceutical Co., Ltd., grants, personal fees and other from Takeda Pharmaceutical Co.,Ltd., grants and personal fees from Taiho Pharmaceutical Co.,Ltd., grants and personal fees from Symbio Pharmaceuticals Limited., personal fees from NANZANDO Co.,Ltd., personal fees from YODOSHA CO., LTD., personal fees from Nikkei Business Publications, Inc, personal fees from Thermo Fisher Scientific K.K., personal fees from YOMIURI TELECASTING CORPORATION., personal fees from Nippon Kayaku Co.,Ltd., grants and personal fees from AbbVie Inc, grants from inVentiv Health Japan, grants from ICON Japan K.K., grants from GRITSONE ONCOLOGY.INC, grants from PAREXEL International Corp., grants from Kissei Pharmaceutical Co.,Ltd., grants from EPS Corporation., grants from Syneos Health., grants from Pfizer R&D Japan G.K., grants from A2 Healthcare Corp., grants from Quintiles Inc. / IQVIA Services JAPAN K.K., grants from EP-CRSU CO., LTD., grants from Linical Co.,Ltd., grants from Eisai Co., Ltd., grants from CMIC Shift Zero K.K., grants from Kyowa Hakko Kirin Co.,Ltd, grants from Bayer Yakuhin, Ltd, grants from EPS International Co.,Ltd.,, grants from Otsuka Pharmaceutical Co., Ltd., outside the submitted work; . RK has received lecture fees from Bristol-Myers Squibb Co. Ltd.; and honoraria from Eli Lilly Japan K.K. K. E. Somers, K. Furuuchi, and T. Uenaka are employees of Eisai Inc. TT and YO declare no potential conflicts of interest.

DATA AVAILABILITY STATEMENT

All data that support the findings of this study are available from the corresponding author upon reasonable request.

ORCID

Hisato Kawakami  <https://orcid.org/0000-0002-3280-4850>

Yuta Onodera  <https://orcid.org/0000-0002-0152-6560>

REFERENCES

1. Bray F, Ferlay J, Soerjomataram I, et al. Global cancer statistics 2018: gLOBOCAN estimates of incidence and mortality worldwide for 36 cancers in 185 countries. *CA Cancer J Clin.* 2018;68:394-424.

2. Chen C, Ke J, Zhou XE, et al. Structural basis for molecular recognition of folic acid by folate receptors. *Nature*. 2013;500:486-489.
3. Parker N, Turk MJ, Westrick E, et al. Folate receptor expression in carcinomas and normal tissues determined by a quantitative radioligand binding assay. *Anal Biochem*. 2005;338:284-293.
4. Scaranti M, Cojocaru E, Banerjee S, et al. Exploiting the folate receptor α in oncology. *Nat Rev Clin Oncol*. 2020;9:020-0339.
5. Kim M, Pyo S, Kang CH, et al. Folate receptor 1 (FOLR1) targeted chimeric antigen receptor (CAR) T cells for the treatment of gastric cancer. *PLoS One*. 2018;13:e0198347-e0198347.
6. Cheng X, Li J, Tanaka K, et al. MORAb-202, an Antibody-Drug Conjugate Utilizing Humanized Anti-human FR α Farletuzumab and the Microtubule-targeting Agent Eribulin, has Potent Antitumor Activity. *Mol Cancer Ther*. 2018;17:2665-2675.
7. Liu Y, Lian T, Yao Y. A systematic review and meta-analysis of higher expression of folate receptor alpha (FOLR1) predicts poor cancer prognosis. *Biomarkers*. 2020:1-8.
8. Moll UM, Petrenko O. The MDM2-p53 interaction. *Mol Cancer Res*. 2003;1:1001-1008.
9. Ganguli G, Wasylyk B. p53-independent functions of MDM2. *Mol Cancer Res*. 2003;1:1027-1035.
10. Nicholson J, Scherl A, Way L, et al. A systems wide mass spectrometric based linear motif screen to identify dominant in-vivo interacting proteins for the ubiquitin ligase MDM2. *Cell Signal*. 2014;26:1243-1257.
11. Yang J, Li B, He QY. Significance of prohibitin domain family in tumorigenesis and its implication in cancer diagnosis and treatment. *Cell Death Dis*. 2018;9:018-0661.
12. Chen Y, Wang DD, Wu YP, et al. MDM2 promotes epithelial-mesenchymal transition and metastasis of ovarian cancer SKOV3 cells. *Br J Cancer*. 2017;117:1192-1201.
13. Yang W, Dolloff NG, El-Deiry WS. ERK and MDM2 prey on FOXO3a. *Nat Cell Biol*. 2008;10(2):125-126. <https://doi.org/10.1038/ncb0208-125>.
14. Zhang Z, Wang H, Li M, et al. MDM2 is a negative regulator of p21WAF1/CIP1, independent of p53. *J Biol Chem*. 2004;279:16000-16006.
15. Uchida C, Miwa S, Kitagawa K, et al. Enhanced Mdm2 activity inhibits pRB function via ubiquitin-dependent degradation. *Embo J*. 2005;24:160-169.
16. Zhang Z, Wang H, Li M, et al. Stabilization of E2F1 protein by MDM2 through the E2F1 ubiquitination pathway. *Oncogene*. 2005;24:7238-7247.
17. Koster R, Timmer-Bosscha H, Bischoff R, et al. Disruption of the MDM2-p53 interaction strongly potentiates p53-dependent apoptosis in cisplatin-resistant human testicular carcinoma cells via the Fas/FasL pathway. *Cell Death Dis*. 2011;2:33.
18. Bagrodia A, Lee BH, Lee W, et al. Genetic Determinants of Cisplatin Resistance in Patients With Advanced Germ Cell Tumors. *Journal of Clinical Oncology*. 2016;34:4000-4007.
19. Ebel W, Routhier EL, Foley B, et al. Preclinical evaluation of MORAb-003, a humanized monoclonal antibody antagonizing folate receptor-alpha. *Cancer Immun*. 2007;7:6.
20. Tamura N, Fujiwara Y, Hashimoto T, et al. Correlation between the expression of folate receptor alpha (FR α) and clinicopathological features in patients with lung adenocarcinoma. *Lung Cancer*. 2020;145:152-157.
21. Sun P, Dong P, Dai K, et al. p53-Independent Role of MDM2 in TGF- β 1 Resistance. *Science*. 1998;282:2270-2272.
22. Nijtmans LG, Artal SM, Grivell LA, et al. The mitochondrial PHB complex: roles in mitochondrial respiratory complex assembly, ageing and degenerative disease. *Cell Mol Life Sci*. 2002;59:143-155.
23. Lin J, Spidel JL, Maddage CJ, et al. The antitumor activity of the human FOLR1-specific monoclonal antibody, farletuzumab, in an ovarian cancer mouse model is mediated by antibody-dependent cellular cytotoxicity. *Cancer Biol Ther*. 2013;14:1032-1038.
24. Yoshida T, Ozawa Y, Kimura T, et al. Eribulin mesilate suppresses experimental metastasis of breast cancer cells by reversing phenotype from epithelial-mesenchymal transition (EMT) to mesenchymal-epithelial transition (MET) states. *Br J Cancer*. 2014;110:1497-1505.

SUPPORTING INFORMATION

Additional supporting information may be found online in the Supporting Information section at the end of the article.

How to cite this article: Sakai H, Kawakami H, Teramura T, et al. Folate receptor α increases chemotherapy resistance through stabilizing MDM2 in cooperation with PHB2 that is overcome by MORAb-202 in gastric cancer. *Clin Transl Med*. 2021;11:e454. <https://doi.org/10.1002/ctm2.454>